Water Supply

IWA PUBLISHING

Water Supply Vol 22 No 8, 6728 doi: 10.2166/ws.2022.282

The transformation mechanism of ofloxacin (OFL) by chlorine dioxide disinfection in water distribution system: kinetics, byproducts and toxicity

Peng Chen[a], Shaowei Hu[a], Guangyu Ma[a], Fei Wang[a], Fang Liu[a], Yong Wang[a] and Guilin He[b,*]

[a] Ansteel Iron & Steel Research Institutes, Anshan 114009, China
[b] School of Municipal and Environmental Engineering, Shandong Jianzhu University, Jinan 250101, China
*Corresponding author. E-mail: glhe@zju.edu.cn

GH, 0000-0002-5067-7736

ABSTRACT

There is a research gap on the transformation of ofloxacin (OFL) in water supply systems under the action of ClO_2. The degradation kinetics of OFL under different ClO_2 concentrations, pH and pipe materials, and formation of intermediates, as well as the toxicity of water in water supply systems were first studied. The results showed that the degradation of OFL in PE pipe and deionized water increased with the increase of ClO_2 concentration, and the reaction of OFL followed the second-order kinetic model. The removal rate of OFL in deionized water was faster than that in PE pipe. The degradation rate of OFL in PE tube and deionized water were positively correlated with pH. In addition, degradation efficiency of OFL in different pipes followed: cast iron pipe > stainless steel pipe > PE pipe. The detection of OFL intermediates showed that the cleavage of piperazine groups were the main and initial products in the degradation process of OFL. In addition, the decarboxylation intermediates of quinolone groups were also detected. The aquatic toxicity test showed that the degradation of OFL by ClO_2 would increase the toxicity of water, therefore, the decrease of OFL may not mean the decrease of water toxicity.

Key words: chlorine dioxide, ofloxacin, pipe material, toxicity, transformation mechanism

HIGHLIGHTS

- In this study, the degradation of OFL in pilot-scale PE pipe was detected for the first time.
- The oxidation rate of OFL was higher in deionized water than in PE pipe
- The oxidation of OFL by ClO_2 would increase the potential risk of water quality safety.

GRAPHICAL ABSTRACT

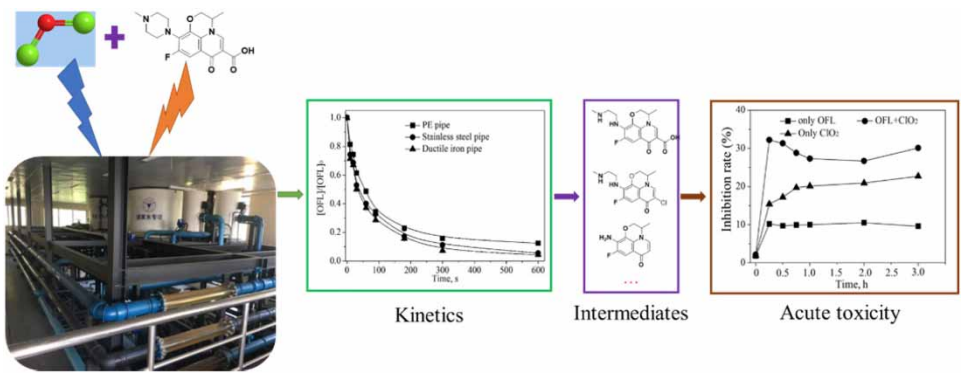

1. INTRODUCTION

Chlorine disinfection is currently the most cost-effective and widely used drinking water disinfection process for water supply systems (Gallard & von Gunten 2002; Gao *et al.* 2018). However, this inevitably produces halogenated disinfection

byproducts that are harmful to humans, such as trihalomethanes (THMs) and haloacetic acids (HAAs) (Sharma *et al.* 2014). The US Environmental Protection Agency (EPA) has defined the maximum content of THMs and HAAs in drinking water as 80 μg/L and 60 μg/L, respectively (Ruecker *et al.* 2017). In recent years, following increasing research on the hazards of traditional chlorination disinfection byproducts and to meet the drinking water quality standards for THMs and HAAs, ClO_2 disinfection technology has received increasing attention (Volk *et al.* 2002; Lv *et al.* 2021). ClO_2 results in rapid and efficient sterilization and reduces the generation of halogenated disinfection byproducts (Navalon *et al.* 2008; Sorlini *et al.* 2014).

Fluoroquinolone antibiotics (FQs) are a class of broad-spectrum antibacterials that are widely used to treat diseases in humans and animals (Xu *et al.* 2015; Guo *et al.* 2017; Castrignanò *et al.* 2020). However, after ingestion, they cannot be completely absorbed and some FQs can be excreted as technical components or active metabolites and enter into the sewage system (Tong & Xiang 2007; Lastre-Acosta *et al.* 2019). Traditional wastewater treatment systems are not able to remove FQs efficiently, resulting in the migration of FQs among environmental media such as sewage plants, surface water, and groundwater, ultimately affecting systems of drinking water treatment (Yahya *et al.* 2014; Annabi *et al.* 2016; Y. Jia *et al.* 2018). An investigation conducted by Ye *et al.* (2007) found that FQ antibiotics in finished water in North Carolina were present at a concentration of 1.2–4.0 ng/L. In addition, the detection rates of FQ antibiotics in the drinking water of Guangzhou and Macau in China have been determined to be as high as 77.5% and 100%, respectively. The contamination of FQs in drinking water mainly comes from the incomplete treatment of FQs in drinking water plants. The long-term consumption of water containing FQs can lead to an increased risk of drug resistance in humans and other organisms (Clark *et al.* 2001; Janecko *et al.* 2016). Therefore, when ClO_2 is used for disinfection, the transformation mechanism of residual FQs in water supply systems remains to be further studied, so as to ensure the safety of drinking water.

Ofloxacin (OFL) is a third-generation FQ antibiotic, mainly used for urinary infections, upper respiratory tract infections, and gastrointestinal infections caused by sensitive bacteria (Yassine *et al.* 2017; Wang *et al.* 2019). OFL contains a quinolone ring in its chemical structure, which can be removed by oxidation with a variety of oxidizing agents including manganese dioxide, ozonation, ferrates, and chlorine (Sharma 2008; Carbajo *et al.* 2015; Yassine *et al.* 2017). However, most current studies on OFL have focused on simple reaction environments, such as beakers of deionized water or organic solvents. The study of the migration and transformation of residual OFL in the water supply network under the action of ClO_2 has not yet been reported. Different pipes, flow rates, temperatures, and other factors in the actual water supply network can affect the decay of ClO_2 and the reaction rate between ClO_2 and pollutants (He *et al.* 2019; Li *et al.* 2019). For example, in the study of the degradation of fleroxacin (FLE) and chloramphenicol (CAP) by ClO_2 in different pipes, results have shown that the degradation of FLE or CAP has an obvious difference in various pipes (He *et al.* 2019; Li *et al.* 2019). The differences in results obtained in a simple reaction environment would be more notable than those in an actual water supply system. Therefore, this study systematically investigated the transformation mechanism of residual OFL in a water supply system under the action of ClO_2. According to the previous study of degradation of OFL by other oxidants (Liu *et al.* 2020), both OFL and its intermediate products have acute toxicity, and so the acute toxicity during OFL degradation by ClO_2 in this study was also studied.

The details of this study include the following: (i) examining the effects of ClO_2 concentration, pH, and pipe materials on OFL degradation by ClO_2; (ii) identifying the production of OFL intermediates under the action of ClO_2 and elucidating the transformation mechanism; (iii) analyzing the generation of disinfection byproducts; (iv) assessing the actual toxicity during OFL degradation by ClO_2.

2. MATERIALS AND METHODS

2.1. Reagents and materials

All chemicals were obtained from various manufacturers and were used directly without further purification. OFL with a purity of 98%, methanol, acetonitrile and MTBE were purchased from Aladdin Reagent Company (Shanghai, China). Sodium hypochlorite, sodium hydroxide, phosphoric acid, sodium thiosulfate and ascorbic acid were provided by Sinopharm Reagent Company (Shanghai, China). THMs standard and HAAs standard with gas-chromatographically pure mixture were obtained from Cansyn (Toronto, Canada).

2.2. Experimental method

The OFL degradation experiments were carried out both in deionized water and in the pilot-scale water supply system, respectively. The pilot-scale pipe network consists of three loops, which are ductile iron pipe, PE pipe and stainless steel pipe (Figure S1). Before the start of the experiment, the pipe and the dosing pump were cleaned with fresh tap water for about 30 minutes. When the cleaning was completed, the cleaning water was drained, and fresh tap water was injected again to start the experiment. The characteristics of fresh tap water were measured each day, with results given in Table S1. The experimental parameters such as flow rate and water temperature were adjusted to the set values by the automatic adjustment system set on the water supply system. Appropriate amounts of phosphoric acid or NaOH solution were added to the water supply system through the dosing pump to adjust the pH, and then the ClO_2 solution and OFL solution were added to the pipe network in turn to start the experiment. The active ClO_2 stock solutions were prepared based on the hydrochloric acid method by mixing hydrochloric acid with sodium chlorite ($NaClO_2$) to the desired concentrations, and the purity was more than 99%. After the experiment, the concentration of OFL at different times was measured by high performance liquid chromatography (HPLC). In order to reduce accidental errors and ensure the reliability of experimental results, each group of experiments was repeated three times.

2.3. Analytical procedures

The OFL concentration changes during the degradation process were detected by HPLC (Agilent 1200, Santa Clara, CA, USA). The detector was a UV detector with a wavelength of 293 nm. The column temperature was 30 °C and the ratio of mobile phase A (0.5% phosphoric acid) and mobile phase B (methanol) was 75:25 with a flow rate of 1 mL/min. Table S2 lists the limit of detection (LOD) and limit of quantification (LOQ) for OFL. Before the detection of intermediates of OFL oxidation by ClO_2, the water samples were enriched and concentrated by solid-phase extraction. Addition in turn of 6 mL of methanol and 6 mL of deionized water activated the CNWBOND HC-18 SPE (500 mg/3 mL) extraction column. A 1,000 mL water sample flowed through the extraction cartridge at a flow rate of 5 mL/min. After the sample passed, 6 mL of methanol was added to elute the extraction cartridge. The eluate was then blown dry with nitrogen at 45 °C, and then 1 mL of methanol was added to collect oxidation products. The samples were detected by LC-MS (Agilent 6460, Santa Clara, CA, USA). The LC-MS detection conditions were as follows: the chromatographic column model was a Zorbax SB-18 column (2.4 mm × 150 mm, 5 μm). The chromatographic conditions were mobile phase A (0.2% formic acid) and phase B (acetonitrile), using gradient elution: 0–5 min 20% B, 15 min 35% B, 20 min 80% B, 20 –23 min 100% B at a flow rate of 0.3 mL/min. The ionization mode was positive ion electrospray ionization (Electrospray Ionization ESI+), with carrier gas temperature 350 °C, flow rate of 10 mL/min, scanning range of 50–500, pressure of 25 psig, fragmentor voltage of 110 eV, capillary voltage of 4,000 V.

THMs were detected by GC-ECD (GC-450, Varian, Palo Alto, CA, USA). Column type was HP-5 (30 m × 0.32 mm × 0.25 mm), and the injection mode was split with an inlet temperature of 210 °C and injection volume of 3 μL. The detector temperature was 290 °C, while the heating program was as follows: 35 °C for 13 min, then keep at 30 °C/min to 200 °C for 3 min. Makeup gas flow rate was 30 mL/min, and the carrier gas was high-purity nitrogen with a flow rate of 1 mL/min. The method detection limits and recovery for THMs are provided in Table S3(a).

Before the analysis of HAAs, MTBE liquid–liquid extraction was used to pretreat the water samples, and then GC (Varian, Palo Alto, CA, USA) was used for detection. The column model was an HP-5 capillary column (15 m × 0.25 mm × 0.25 μm, Agilent). The injection method was headspace injection/splitless injection, and the detector temperature was 300 °C. The injection port temperature was 175 °C, with an injection volume of 1 μL. The heating program was as follows: 40 °C for 5 min, then 10 °C/min to 140 °C, followed by 25 °C/min to 190 °C, and hold for 0.5 min. The makeup gas flow rate was 30 mL/min. Carrier gas was high-purity nitrogen, with a flow rate of 1 mL/min. The method detection limits and recovery for HAAs are provided in Table S3(b).

The concentrations of ClO_2 were measured by spectrophotometry, using a DR-2800 spectrophotometer (HACH, Loveland, CO, USA). The chlorite in the water sample was detected by ion chromatograph (Dionex ICS-2000, Sunnyvale, CA, USA). The total organic carbon (TOC) of tap water in the pilot-scale pipe was detected by a TOC analyzer (Shimadzu, Kyoto, Japan) (Dong *et al.* 2017). The acute toxicity of water samples collected at different reaction times during OFL oxidation by ClO_2 were evaluated based on the luminescence inhibition of *Vibrio fischeri* bacteria. The luminescence inhibition was detected by a Microtox® Model 500 comprehensive toxicity detector (Strategic Diagnostics Inc., Newark, DE, USA).

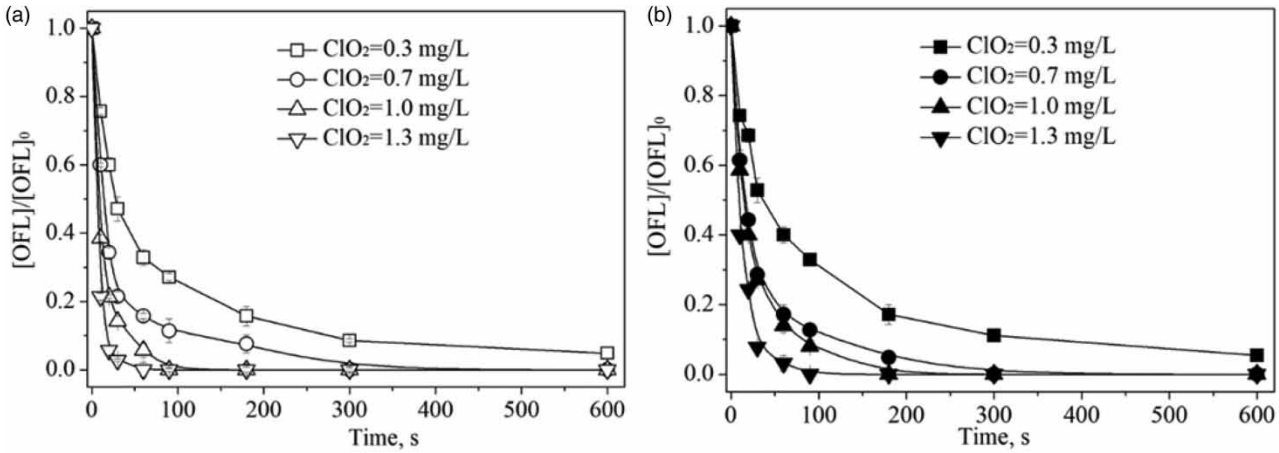

Figure 1 | Oxidation of ofloxacin (OFL) by ClO_2 in (a) deionized water; (b) PE pipe at different ClO_2 concentrations, temperature of 20 ± 2 °C, pH of 7.4 ± 0.2, and [OFL] = 100 μg/L.

3. RESULTS AND DISCUSSION

3.1. OFL oxidation kinetics during ClO_2 treatment

3.1.1. ClO_2 concentration

The degradation of OFL by ClO_2 (0.3–1.3 mg/L) in deionized water and PE pipe were investigated at an initial OFL concentration of 100 μg/L, with a temperature of 20 ± 2 °C, and pH = 7.4 ± 0.2. The results are shown in Figure 1.

As seen from Figure 1, the degradation rate of OFL in both deionized water and PE pipes accelerated with an increasing ClO_2 concentration. When the initial ClO_2 concentration was 0.3 mg/L, the degradation efficiencies of OFL in deionized water and PE pipe, after 90 s of reaction, were 73% and 68%, respectively. When the initial chlorine concentration was increased to 1.3 mg/L and the reaction was performed for 90 s, the degradation rate was 100% in both deionized water and PE pipes. In addition, the degradation rate of OFL in deionized water was higher than that in PE pipe. This was mainly owing to the organic matter, pipe scale, and biofilm of the pipe-wall consuming part of the ClO_2, which made the proportion of ClO_2 used for OFL degradation in PE pipe decrease. In addition, within the selected concentration of ClO_2 in this study, OFL can be effectively removed by 600 s reaction, indicating that OFL degradation mainly occurs at the beginning of the system.

The degradation data of OFL in deionized water and PE pipe at different ClO_2 concentrations were fitted with a first-order kinetics model, and the results are shown in Figure 2. The $\ln([OFL]/[OFL]_0)$ showed a good linear correlation with time ($R^2 > 0.94$). Therefore, the reaction of OFL with ClO_2 was consistent with pseudo-first-order reaction kinetics and the degradation could be expressed by Equation (1):

$$\frac{d(OFL)}{dt} = -k_{obs}[OFL] \tag{1}$$

where k_{obs} is the total reaction rate constant of the reactions, s^{-1}; and [OFL] is the concentration of OFL at different reaction moments, μg/L.

The decay of ClO_2 in deionized water and PE pipe at various ClO_2 concentrations is shown in Figure S2. The results show that the concentration of ClO_2 decreased with the increase of reaction time. A linear fitting of the pseudo-first-order reaction kinetic constants with the ClO_2 concentration at different ClO_2 concentrations was performed, and the results are shown in Figure 3. There was a good linear relationship between the pseudo-first-order reaction kinetics constants and the ClO_2 concentration ($R^2 > 0.93$). Therefore, it could be considered that the degradation of OFL under the action of ClO_2 is consistent with the total reaction rate constant of the reactions, k_{obs}. The relationship between k_{obs} and the ClO_2 concentration could be

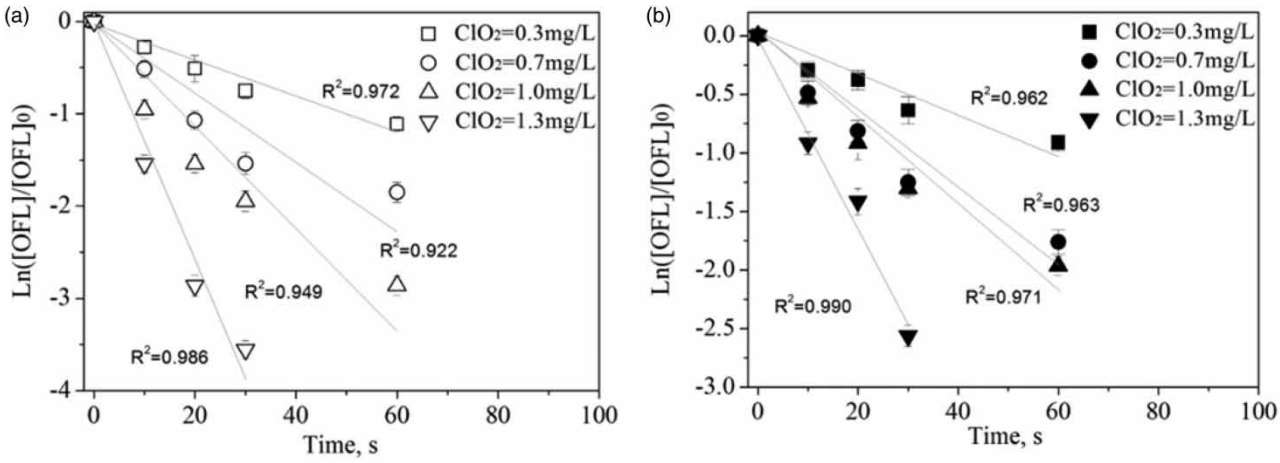

Figure 2 | The relationship of $\ln([OFL]/[OFL]_0)$ with time under different ClO_2 in (a) deionized water and (b) PE pipe at 20 ± 2 °C, pH of 7.4 ± 0.2, and [OFL] = 100 μg/L.

expressed by Equation (2) as follows:

$$k_{obs} = k_c[ClO_2] \tag{2}$$

where k_c is the second-order rate constant, $M^{-1}s^{-1}$; and $[ClO_2]$ is the initial concentration of ClO_2, mg/L.

To investigate the influence of organic matter in tap water, OFL degradation by ClO_2 was carried out by placing tap water from the PE pipe in a beaker (curve B) and the result was compared with the degradation in deionized water (curve A) and PE pipe (curve C). The energy value (velocity gradient) was controlled though stirring of the water in the beaker by a magnetic stirrer to ensure the hydraulic state in the beaker was similar to that in the PE pipe. As shown in Figure 4, the degradation of OFL by ClO_2 followed the order of curve A > curve B > curve C, which means the organic matter in tap water can decrease the degradation of OFL by competing with OFL for ClO_2. However, the influence of this factor was not significant, which might be because of the short reaction time of OFL degradation by ClO_2.

3.1.2. pH

The degradation of OFL at different pH in deionized water and PE pipe was investigated at an initial ClO_2 concentration of 0.3 mg/L, with an initial OFL concentration of 100 μg/L, and a temperature of 20 ± 2 °C. The results are shown in Figure 5.

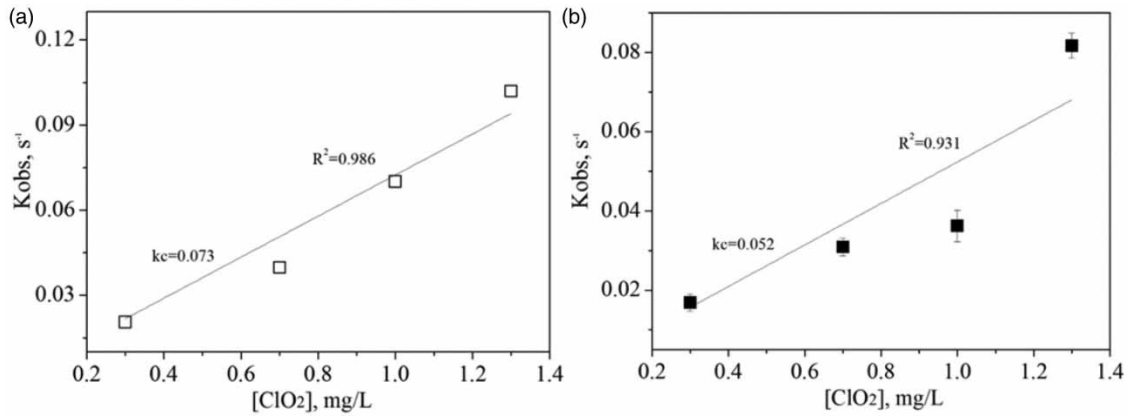

Figure 3 | The relationship of $\ln([OFL]/[OFL]_0)$ with different initial ClO_2 in (a) deionized water and (b) PE pipe at 20 ± 2 °C, pH of 7.4 ± 0.2, and [OFL] = 100 μg/L.

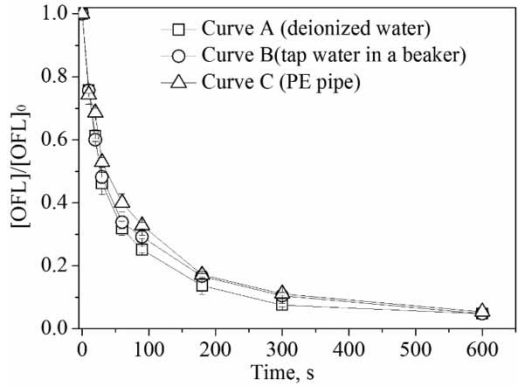

Figure 4 | Oxidation of ofloxacin (OFL) by ClO_2 in deionized water, PE pipe and tap water in a beaker at ClO_2 concentration of 0.3 mg/L, temperature of 20 ± 2 °C, pH of 7.4 ± 0.2, and [OFL] = 100 μg/L.

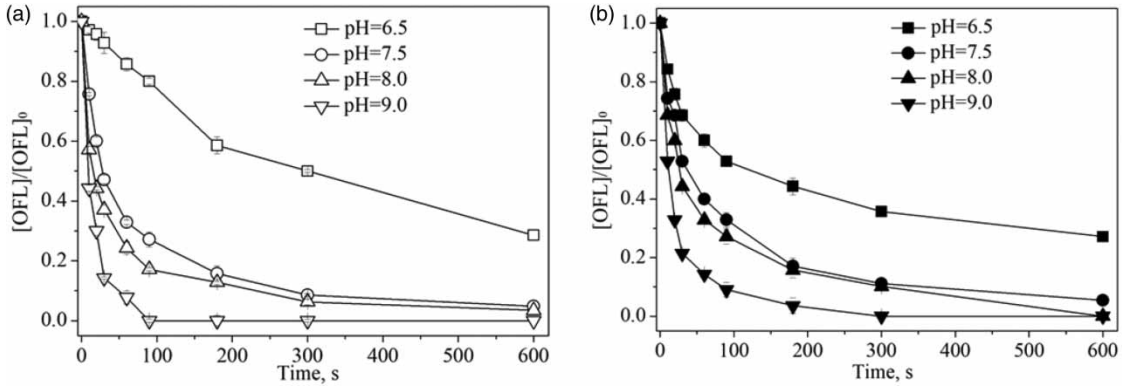

Figure 5 | Oxidation of ofloxacin (OFL) by ClO_2 in (a) deionized water; (b) PE pipe at different pH, temperature of 20 ± 2 °C, pH of 7.4 ± 0.2, $[ClO_2]$ = 0.3 mg/L and [OFL] = 100 μg/L.

The results show that the degradation rate of OFL increased continuously with an increase of pH both in deionized water and PE pipe, which is consistent with the results of previous studies performed on the degradation of other types of FQs by ClO_2. The pH affects the speciation of OFL and ClO_2. OFL can exist in three forms: $OFLH^+$, OFL, and OFL^- (Equation (3)) (Liu *et al.* 2013). With the increase of pH, the proportion of OFL^- increased, and compared with $OFLH^+$ and OFL, OFL^- is more likely to react with ClO_2. Therefore, the degradation rate of OFL increased with the increase of pH. On the other hand, ClO_2 can remain morphologically stable over a wide pH range (2–14) (X. H. Jia *et al.* 2018). Thus, with an increasing pH, the presence of ClO_2 and OFL leads to an increase in OFL degradation. In addition, according to the nonlinear least squares method, the second-order rate constant for the reaction of ClO_2 with OFL^- was $5.81 \times 10^2\ M^{-1}\ s^{-1}$, whereas the second-order rate constant for the reaction of ClO_2 with OFL was $7.34\ M^{-1}\ s^{-1}$, indicating that the reaction of ClO_2 with OFL^- was the main reaction in the system.

$$[OFLH^+] \overset{K_{a1}=5.77}{\Longleftrightarrow} [OFL] \overset{K_{a2}=8.44}{\Longleftrightarrow} [OFL^-] \tag{3}$$

3.1.3. Pipe materials

The degradation of OFL in three types of pipes, namely ductile iron pipe, PE pipe, and stainless steel pipe, was examined at an initial ClO_2 concentration of 0.3 mg/L, with an initial OFL concentration of 100 μg/L, as well as a temperature of 20 ± 2 °C, and pH = 7.4 ± 0.2. As shown in Figure 6, the degradation rate of OFL in the three different pipes was ductile iron pipe > stainless steel pipe > PE pipe. The degradation efficiencies of OFL in ductile iron, stainless steel, and PE pipes were 93%, 89%, and 84%, respectively, after 300 s of reaction.

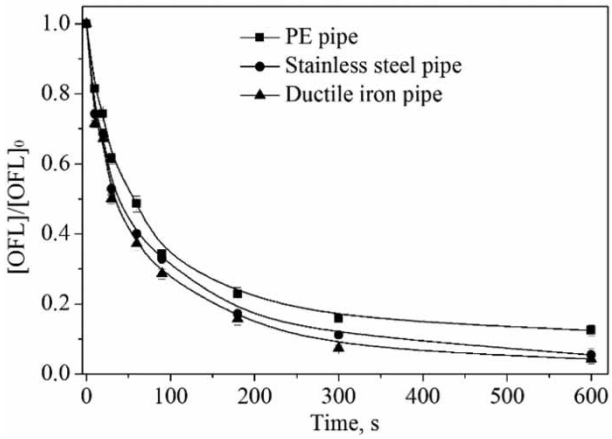

Figure 6 | Oxidation of ofloxacin (OFL) by ClO_2 in different pipes at temperature of 20 ± 2 °C, pH of 7.4 ± 0.2, $[ClO_2] = 0.3$ mg/L and $[OFL] = 100$ μg/L.

As can be seen from the visible pipe section of the pipe system (Figure S3), the pipe scale in the three pipe networks was as follows: stainless steel pipe ≈ PE pipe > ductile iron pipe. The pipe scale contains corroded metals, solid metal oxides, metal ions, biofilms, and natural organic matter, and all of these factors can contribute to the consumption of oxidants. In this case, the ClO_2 consumed by the pipe wall in the three pipe networks was in the following order: stainless steel pipe ≈ PE pipe > ductile iron pipe. In addition, it was found that the organic concentrations of the ductile iron pipe, PE pipe, and stainless steel pipe were 2.37 mg/L, 3.38 mg/L, and 3.09 mg/L, respectively. Therefore, the ClO_2 content available for OFL degradation in ductile iron pipes was higher than that of PE pipe and stainless steel pipe. Furthermore, the concentrations of iron in the water samples extracted from stainless steel pipe and ductile iron pipe were 0.27 mg/L and 0.14 mg/L, respectively, whereas the PE pipe water samples were found to contain no iron ions. Fe^{2+} can be oxidized into Fe^{3+}, and the free radicals generated during the iron oxidation can promote OFL degradation in stainless steel pipe and ductile iron pipe (Dong *et al.* 2017). Comprehensively considering pipe scale, the organic matter in the main water bodies, and the effect of iron on OFL degradation, it should be noted that OFL degradation was fastest in ductile iron pipe, followed by that in stainless steel pipe, and it was slowest in PE pipe.

3.2. Formation of byproducts during OFL oxidation by ClO_2

3.2.1. Identification of intermediates

The OFL degradation in PE pipe was examined at an initial ClO_2 concentration of 1.0 mg/L and an initial OFL concentration of 250 μg/L. Eight intermediates were identified by LC-MS analysis under the action of ClO_2.

Based on the detected intermediates, the proposed transformation pathway of OFL under the action of ClO_2 was speculated, and this is shown in Figure 7. As shown in Figure 7, the piperazine group in the OFL molecule undergoes decarboxylation, defluorination, and substitution reactions simultaneously or sequentially during the oxidation by ClO_2. In addition, the cleavage of the piperazine-based ring is the key and initial reaction step in the entire degradation process. Similar reaction processes have been observed during the degradation of other types of FQs (e.g., CIP, NOR, and ENR) under the action of chlorine, ClO_2, and Fenton reactions (Wang *et al.* 2010; Guo *et al.* 2017; Ling *et al.* 2017). The structure of OFL shows that C2(α-C) and C3(β-C) in the piperazine group of OFL are each attached to a heteroatom (N1 and N4) (Figure 7), which can induce the 'oxidative fragmentation' reaction (Dennis *et al.* 1967), leading to the fracture of C2(α-C) and C3(β-C) under the action of ClO_2. Therefore, during the degradation of OFL, N4 on the piperazine group is attacked first and loses an electron, forming a radical centered on N4. The radical continues to be attacked by ClO_2 in aqueous solution, resulting in the loss of an electron from the N1 atom in the piperazine group and forming a divalent piperazine cation with both N1 and N4 atoms of the piperazine group carrying a positive charge. The divalent piperazine cation is an extremely unstable structure that leads to the cleavage of C2 and C3, resulting in the formation of an imine intermediate, which is rapidly hydrolyzed to produce the dealkylation product OP-335. Subsequently, the intermediate product OP-335 further undergoes two different oxidation processes as shown in Figure 7.

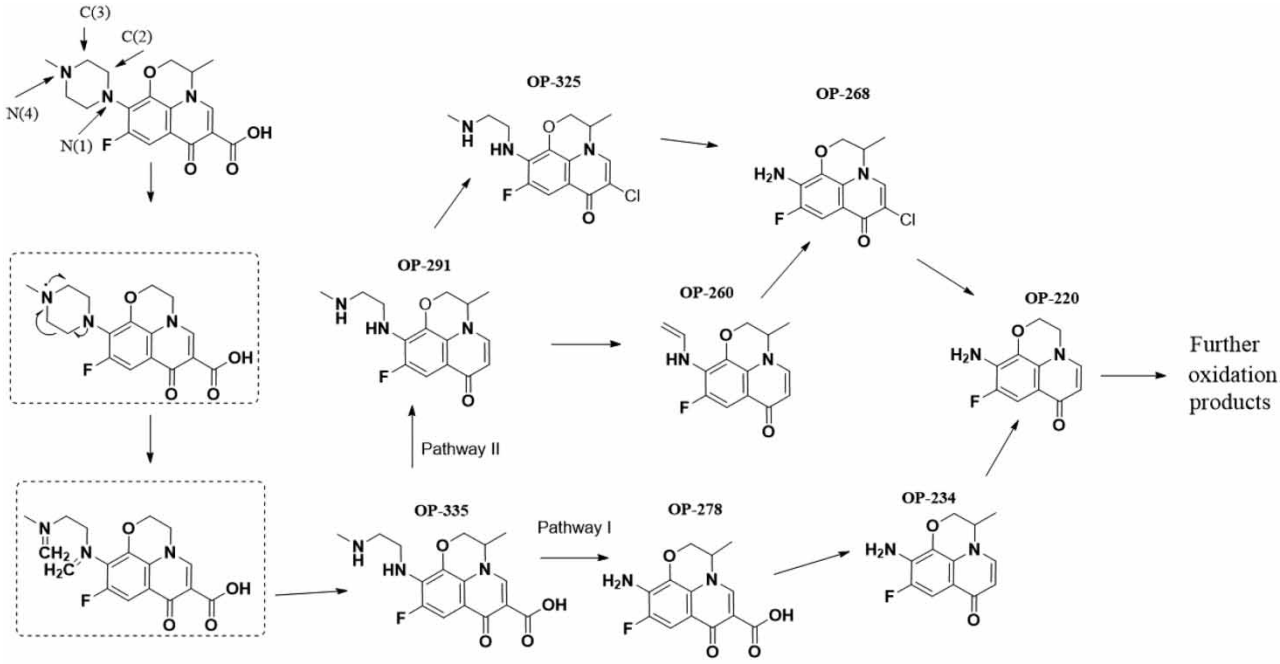

Figure 7 | The proposed transformation pathways of ofloxacin (OFL) oxidation by ClO_2 in PE pipe at temperature of 20 ± 2 °C, pH 7.4 ± 0.2, $[ClO_2] = 1.0$ mg/L, and [OFL] = 250 μg/L.

In pathway I, the piperazine group of OP-335 first undergoes the fracture and removal of ammonia nitrogen and alkyl ($-C_3H_7N$) to produce the intermediate OP-278. Subsequently, the intermediate OP-278 undergoes decarboxylation and dealkylation to produce the product OP-220. In addition to that in pathway I, the intermediate product OP-335 can undergo decarboxylation, degradation of the piperazine group, defluorination, and chlorine substitution reactions. The intermediate P-291 is the product of the decarboxylation of P-325 catalyzed by the N4 of the piperazine group. Subsequently, the hydrogen atom on the quinolone group of the intermediate OP-291 is replaced by a chlorine atom via halogenated decarboxylation to form OP-325. Then, the piperazine group in the intermediate P-325 is further oxidized to produce P-268. In addition, OP-291 can generate OP-260 via the removal of ammonia nitrogen and alkyl on the piperazine group. Finally, the product P-268 undergoes sequential dealkylation to produce the compound P-220.

3.2.2. Formation of halogenated DBPs and chlorite

The generation of halogenated DBPs and chlorite during the degradation of OFL in PE pipe was investigated at an initial ClO_2 concentration of 1.0 mg/L and an initial OFL concentration of 250 μg/L. In addition, a blank control group with only the addition of ClO_2 was used. The results are shown in Figure 8. From Figure 8(a), it can be seen that the generation trends of the three THMs in the presence or absence of OFL have little difference, and the generation of THMs was mainly concentrated in the first 1 h of the reaction. After 1 h of the reaction, the concentrations of THMs during OFL oxidation and those in the blank control group were 21.38 μg/L and 20.97 μg/L, respectively. This indicates that the oxidation of OFL by ClO_2 has little contribution to the formation of THMs. This conclusion also applies to the study of the formation trend of HAAs in this experiment.

The process of chlorite generation during OFL oxidation under the action of ClO_2 is shown in Figure 9. It can be seen that the concentration of chlorite increased rapidly within the first hour of the reaction. After 1 h of the reaction, the concentration of chlorite in the OFL system for chlorine dioxide degradation was 0.309 mg/L. The results indicated that ClO_2 disinfection produces a certain amount of chlorite, which is a drawback of ClO_2 disinfection.

3.2.3. Toxicity assessment of the oxidation of OFL in PE pipe

The acute toxicity of the water during the degradation of OFL was examined using experimental conditions consistent with those of the analysis of the intermediates. Meanwhile, two groups of blank control tests were set up as follows: (1) only OFL

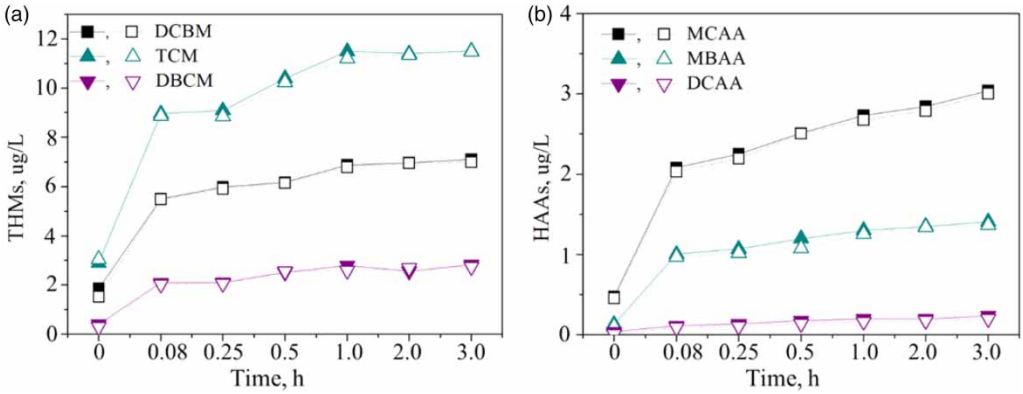

Figure 8 | Formation of (a) trihalomethanes (THMs); (b) haloacetic acids (HAAs) during ofloxacin (OFL) oxidation by ClO_2 and blank experiment in PE pipe. Experimental conditions: temperature 20 ± 2 °C, pH 7.4 ± 0.2, $[ClO_2] = 1.0$ mg/L and [OFL] = 250 μg/L. In the blank experiment, [OFL] = 0 μg/L and the other experiment was same as the OFL oxidation experiment. For each analyte, the solid symbol represents the concentration produced in OFL oxidation, while the open symbol represents the concentration produced in the blank experiment. Abbreviations: DBCM, dibromochloromethane; TCM, chloroform; DCBM, bromodichloromethane; DCAA, dichloroacetic acid; MBAA, monobromoacetic acid; MCAA, monochloroacetic acid.

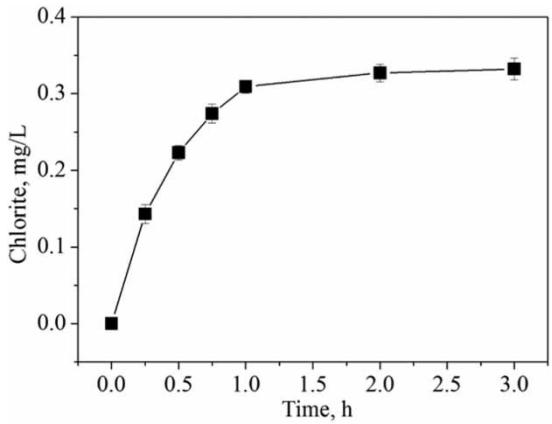

Figure 9 | Formation of chlorite during ofloxacin (OFL) oxidation by ClO_2 in PE pipe at temperature 20 ± 2 °C, pH 7.4 ± 0.2, $[ClO_2] = 1.0$ mg/L and [OFL] = 250 μg/L.

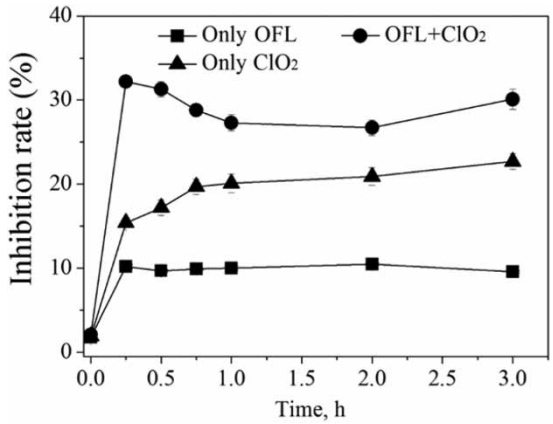

Figure 10 | Inhibition rate of acute toxicity during ofloxacin (OFL) oxidation by ClO_2 in PE pipe at temperature 20 ± 2 °C, pH 7.4 ± 0.2, $[ClO_2] = 1.0$ mg/L and [OFL] = 250 μg/L. Experimental conditions: temperature 20 ± 2 °C, pH 7.4 ± 0.2, $[ClO_2] = 1.0$ mg/L and [OFL] = 250 μg/L. In the blank experiment, [OFL] = 0 μg/L and the other experiment was same as the OFL oxidation experiment.

solution was added without ClO_2 solution (blank experiment A); (2) only ClO_2 was added without OFL solution (blank experiment B). The conditions of the blank experiment were consistent with those of the OFL oxidation experiment, except that no ClO_2 or OFL was added.

The changes in acute toxicity during the experiment are shown in Figure 10. After 15 min of the reaction, the acute toxicity of the water increased rapidly in both OFL degradation and blank experiment B. The acute toxicity of the water with OFL degradation was significantly higher than the toxicity of blank experiment B (only ClO_2). As shown in Figures 7–9, the acute toxicity in the water was mainly caused by the halogenated DBPs and chlorite, as well as by the cleavage of intermediates generated during the initial stages of OFL degradation. From 15 min to 1 h, a significant difference in the inhibition rate of luminescent bacteria between the OFL degradation experiment and blank experiment B was noticed. Within this phase, the inhibition of luminescent bacteria during the degradation of OFL by ClO_2 gradually diminished with time, whereas the inhibition of luminescent bacteria when only ClO_2 was added increased with time. As shown in Figure 7, the changes of acute toxicity during the OFL oxidation experiments might be related to the further transformation of piperazine-group cleavage in intermediates. After 1 h of the reaction, the changes in the inhibition rate were very small in both the OFL oxidation experiment and blank experiment B, which was mainly due to the limited increase in halogenated DBPs at that stage (Figure 8). Furthermore, in comparison with the acute toxicity in blank experiment A (only OFL), both the oxidation of OLF by ClO_2 and blank experiment B (only ClO_2) resulted in an increased inhibition rate of luminescent bacteria, resulting in an increased potential risk to the safety of the water body.

4. CONCLUSIONS

The degradation rates of OFL under the action of ClO_2 in deionized water and PE pipes were positively correlated with the ClO_2 concentration and pH, and the degradation rates in different pipes were as follows: ductile iron pipe > stainless steel pipe > PE pipe. The detection of OFL degradation intermediates showed that the product of piperazine-group cleavage was the initial and the main intermediate. Furthermore, the intermediate of quinolone group decarboxylation was also detected. The contributions of OFL degradation under the action of ClO_2 to the generation of halogenated DBPs and chlorite were limited. OFL degradation by ClO_2 leads to an increase of acute toxicity, indicating that a decrease in OFL concentration might not mean a decrease of toxicity. In the actual water supply, while removing organic pollutants, necessary measures should be taken to reduce the generation of intermediate products during ClO_2 disinfection so as to reduce the toxicity of drinking water.

ACKNOWLEDGEMENTS

This work has been financially supported by the China Postdoctoral Science Foundation (No. 2018M632465) and the Doctoral Research Fund of Shandong Jianzhu University (X20038Z0101).

DATA AVAILABILITY STATEMENT

All relevant data are included in the paper or its Supplementary Information.

CONFLICT OF INTEREST

The authors declare there is no conflict.

REFERENCES

Annabi, C., Fourcade, F., Soutrel, I., Geneste, F., Floner, D., Bellakhal, N. & Amrane, A. 2016 Degradation of enoxacin antibiotic by the electro-Fenton process: optimization, biodegradability improvement and degradation mechanism. *Journal of Environmental Management* **165**, 96–105.

Carbajo, J. B., Petre, A. L., Rosal, R., Herrera, S., Letón, P., García-Calvo, E., Fernández-Alba, A. R. & Perdigón-Melón, J. A. 2015 Continuous ozonation treatment of ofloxacin: transformation products, water matrix effect and aquatic toxicity. *Journal of Hazardous Materials* **292**, 34–43.

Castrignanò, E., Kannan, A. M., Proctor, K., Petrie, B., Hodgen, S., Feil, E. J., Lewis, S. E., Lopardo, L., Camacho-Muñoz, D., Rice, J., Cartwright, N., Barden, R. & Kasprzyk-Hordern, B. 2020 (Fluoro)quinolones and quinolone resistance genes in the aquatic environment: a river catchment perspective. *Water Research* **182**, 116015.

Clark, D. W. J., Layton, D., Wilton, L. V., Pearce, G. L. & Shakir, S. A. W. 2001 Profiles of hepatic and dysrhythmic cardiovascular events following use of fluoroquinolone antibacterials: experience from large cohorts from the drug safety research unit prescription-event monitoring database. *Drug Safety* **24**, 1143–1154.

Dennis, W. H., Hull, L. A. & Rosenblatt, D. H. 1967 Oxidations of amines. IV. Oxidative fragmentation. *Journal of Organic Chemistry* **32** (12), 3783–3787.

Dong, F., Li, C., He, G., Chen, X. & Mao, X. 2017 Kinetics and degradation pathway of sulfamethazine chlorination in pilot-scale water distribution systems. *Chemical Engineering Journal* **321**, 521–532.

Gallard, H. & von Gunten, U. 2002 Chlorination of phenols: kinetics and formation of chloroform. *Environmental Science & Technology* **36** (5), 884–890.

Gao, Y., Jiang, J., Zhou, Y., Pang, S. Y., Ma, J., Jiang, C., Yang, Y., Huang, Z. S., Gu, J., Guo, Q., Duan, J. B. & Li, J. 2018 Chlorination of bisphenol S: kinetics, products, and effect of humic acid. *Water Research* **131**, 208–217.

Guo, H., Ke, T., Gao, N., Liu, Y. & Cheng, X. 2017 Enhanced degradation of aqueous norfloxacin and enrofloxacin by UV-activated persulfate: kinetics, pathways and deactivation. *Chemical Engineering Journal* **316**, 471–480.

He, G., Zhang, T., Zheng, F., Li, C., Zhang, Q., Dong, F. & Huang, Y. 2019 Reaction of fleroxacin with chlorine and chlorine dioxide in drinking water distribution systems: kinetics, transformation mechanisms and toxicity evaluations. *Chemical Engineering Journal* **374**, 1191–1203.

Janecko, N., Pokludova, L., Blahova, J., Svobodova, Z. & Literak, I. 2016 Implications of fluoroquinolone contamination for the aquatic environment – a review. *Environmental Toxicology and Chemistry* **35**, 2647–2656.

Jia, X. H., Feng, L., Liu, Y. Z. & Zhang, L. Q. 2018 Degradation behaviors and genetic toxicity variations of pyrazolone pharmaceuticals during chlorine dioxide disinfection process. *Chemical Engineering Journal* **345**, 156–164.

Jia, Y., Khanal, S. K., Shu, H., Zhang, H., Chen, G. H. & Lu, H. 2018 Ciprofloxacin degradation in anaerobic sulfate-reducing bacteria (SRB) sludge system: mechanism and pathways. *Water Research* **136**, 64–74.

Lastre-Acosta, A. M., Barberato, B., Parizi, M. P. S. & Teixeira, A. C. S. C. 2019 Direct and indirect photolysis of the antibiotic enoxacin: kinetics of oxidation by reactive photo-induced species and simulations. *Environmental Science and Pollution Research* **26**, 4337–4347.

Li, C., Luo, F., Duan, H., Dong, F., Chen, X., Feng, M., Zhang, Z., Cizmas, L. & Sharma, V. K. 2019 Degradation of chloramphenicol by chlorine and chlorine dioxide in a pilot-scale water distribution system. *Separation and Purification Technology* **211**, 564–570.

Ling, W., Ben, W., Xu, K., Zhang, Y., Yang, M. & Qiang, Z. 2017 Ozonation of norfloxacin and levofloxacin in water: specific reaction rate constants and defluorination reaction. *Chemosphere* **195**, 252–259.

Liu, Y., Zhang, P., Li, H., Tang, R., Cui, R. R. & Wang, W. 2013 Photochemical properties and phototoxicity of pazufloxacin: a stable and transient study. *Journal of Photochemistry & Photobiology B: Biology* **118**, 58–65.

Liu, X., Liu, Y., Lu, S., Wang, Z., Wang, Y., Zhang, G., Guo, X., Guo, W., Zhang, T. & Xi, B. 2020 Degradation difference of ofloxacin and levofloxacin by UV/H_2O_2 and UV/PS (persulfate): efficiency, factors and mechanism. *Chemical Engineering Journal* **385**, 123987.

Lv, J., Ou, C., Fu, M. & Xu, Z. 2021 Characteristics and transformation pathways of venlafaxine degradation during disinfection processes using free chlorine and chlorine dioxide. *Chemosphere* **276**, 130147.

Navalon, S., Alvaro, M. & Garcia, H. 2008 Reaction of chlorine dioxide with emergent water pollutants: product study of the reaction of three β-lactam antibiotics with ClO_2. *Water Research* **42**, 1935–1942.

Ruecker, A., Uzun, H., Karanfil, T., Tsui, M. T. K. & Chow, A. T. 2017 Disinfection byproduct precursor dynamics and water treatability during an extreme flooding event in a coastal blackwater river in southeastern United States. *Chemosphere* **188**, 90–98.

Sharma, V. K. 2008 Oxidative transformations of environmental pharmaceuticals by Cl_2, ClO_2, O_3, and Fe(VI): kinetics assessment. *Chemosphere* **73**, 1379–1386.

Sharma, V. K., Zboril, R. & McDonald, T. J. 2014 Formation and toxicity of brominated disinfection byproducts during chlorination and chloramination of water: a review. *Journal of Environmental Science & Health, Part B* **49**, 212–228.

Sorlini, S., Gialdini, F., Biasibetti, M. & Collivignarelli, C. 2014 Influence of drinking water treatments on chlorine dioxide consumption and chlorite/chlorate formation. *Water Research* **54**, 44–52.

Tong, C. & Xiang, G. 2007 Sensitive determination of enoxacin by its enhancement effect on the fluorescence of terbium(III)–sodium dodecylbenzene sulfonate and its luminescence mechanism. *Journal of Luminescence* **126** (2), 575–580.

Volk, C. J., Hofmann, R., Chauret, C., Gagnon, G. A., Ranger, G. & Andrews, R. C. 2002 Implementation of chlorine dioxide disinfection: effects of the treatment change on drinking water quality in a full-scale distribution system. *Journal of Environmental Engineering and Science* **1** (5), 323–330.

Wang, P., He, Y. L. & Huang, C. H. 2010 Oxidation of fluoroquinolone antibiotics and structurally related amines by chlorine dioxide: reaction kinetics, product and pathway evaluation. *Water Research* **44**, 5989–5998.

Wang, X., Li, Y., Li, R., Yang, H., Zhou, B., Wang, X. & Xie, Y. 2019 Comparison of chlorination behaviors between norfloxacin and ofloxacin: reaction kinetics, oxidation products and reaction pathways. *Chemosphere* **215**, 124–132.

Xu, Y., Chen, T., Wang, Y., Tao, H., Liu, S. & Shi, W. 2015 The occurrence and removal of selected fluoroquinolones in urban drinking water treatment plants. *Environmental Monitoring and Assessment* **187** (12), 729.

Yahya, M. S., Oturan, N., El Kacemi, K., El Karbane, M., Aravindakumar, C. T. & Oturan, M. A. 2014 Oxidative degradation study on antimicrobial agent ciprofloxacin by electro-fenton process: kinetics and oxidation products. *Chemosphere* **117**, 447–454.

Yassine, M. H., Rifai, A., Hoteit, M., Mazellier, P. & Al Iskandarani, M. 2017 Study of the degradation process of ofloxacin with free chlorine by using ESI-LCMSMS: kinetic study, by-products formation pathways and fragmentation mechanisms. *Chemosphere* **189**, 46–54.

Ye, Z., Weinberg, H. S. & Meyer, M. T. 2007 Trace analysis of trimethoprim and sulfonamide, macrolide, quinolone, and tetracycline antibiotics in chlorinated drinking water using liquid chromatography electrospray tandem mass spectrometry. *Analytical Chemistry* **79** (3), 1135–1144.

First received 4 April 2022; accepted in revised form 22 July 2022. Available online 1 August 2022